

## PUBLISHED VERSION

Lu, D. H.; Saito, K.; Thomas, Anthony William; Tsushima, Kazuo; Williams, Anthony Gordon  
[Electromagnetic form factors of the bound nucleon](#) Physical Review C, 1999; 60(6):068201

© 1999 American Physical Society

<http://link.aps.org/doi/10.1103/PhysRevC.60.068201>

### PERMISSIONS

<http://publish.aps.org/authors/transfer-of-copyright-agreement>

“The author(s), and in the case of a Work Made For Hire, as defined in the U.S. Copyright Act, 17 U.S.C.

§101, the employer named [below], shall have the following rights (the “Author Rights”):

[...]

3. The right to use all or part of the Article, including the APS-prepared version without revision or modification, on the author(s)' web home page or employer's website and to make copies of all or part of the Article, including the APS-prepared version without revision or modification, for the author(s)' and/or the employer's use for educational or research purposes.”

27<sup>th</sup> March 2013

<http://hdl.handle.net/2440/10874>

## Electromagnetic form factors of the bound nucleon

D. H. Lu,<sup>1,2</sup> K. Tsushima,<sup>2</sup> A. W. Thomas,<sup>2</sup> A. G. Williams,<sup>2</sup> and K. Saito<sup>3</sup>

<sup>1</sup>*Department of Physics, National Taiwan University, Taipei 10617, Taiwan*

<sup>2</sup>*Department of Physics and Mathematical Physics and Special Research Centre for the Subatomic Structure of Matter, University of Adelaide, Adelaide, Australia 5005*

<sup>3</sup>*Physics Division, Tohoku College of Pharmacy, Sendai 981-8558, Japan*

(Received 24 July 1998; revised manuscript received 19 July 1999; published 5 November 1999)

We calculate electromagnetic form factors of the proton bound in specified orbits for several closed-shell nuclei. The shell structure of the finite nuclei, together with the internal quark substructure of the nucleon, are self-consistently described by the quark-meson-coupling model. We find that the medium-modified electric and magnetic form factors of the bound nucleon deviate considerably from those of the free nucleon. Our results suggest that this medium correction on the nucleon's quark substructure may be detectable in forthcoming quasielastic electron-nucleus scattering. [S0556-2813(99)00511-7]

PACS number(s): 13.40.Gp, 12.39.Ba, 21.65.+f

Whether or not quark degrees of freedom play any significant role beyond conventional nuclear theory (involving baryons and mesons) is a fundamental question in strong interaction physics. Tremendous effort has been devoted to the study of medium modifications of hadron properties [1]. The idea that nucleons might undergo considerable change of their internal structure in a baryon-rich environment has been stimulated by a number of experiments, e.g., the variation of nucleon structure functions in lepton deep-inelastic scattering off nuclei [2], the quenching of the axial vector coupling constant  $g_A$  in nuclear  $\beta$  decay [3], and the missing strength of the response functions in nuclear quasielastic electron scattering [4]. Though the conventional interpretation arising through polarization effects and other hadronic degrees of freedom ( $\Delta$  excitations, meson exchange currents, etc.) cannot be ruled out at this stage [5,6], it is rather interesting to explore the possibilities of a change in the internal structure of the bound nucleon.

There have been several effective Lagrangian approaches in the literature dealing with modifications of the nucleon size and electromagnetic properties in medium [7,8]. All these investigations found that nucleon electromagnetic form factors are suppressed and the rms radii of the proton somewhat increased in bulk nuclear matter—in addition to hadron mass reductions. In Ref. [8], we examined medium modifications of nucleon electromagnetic properties in nuclear matter, using the quark-meson coupling model (QMC) [9,10]. The self-consistent change in the internal structure of a bound nucleon is consistent with the constraints from  $\gamma$ -scaling data [11] and the Coulomb sum rule [12]. In this paper, we calculate electromagnetic form factors for a nucleon bound in specific, shell-model orbits of realistic finite nuclei. This is of direct relevance to quasielastic electron-nucleus scattering experiments [13].

The details for solving equations of motion of QMC for finite nuclei can be found in Ref. [10]. Here we briefly illustrate the essential features related to this work. For the calculation of the nucleon shell-model wave functions, the QMC model for spherical finite nuclei, in the mean-field approximation, can be summarized in an effective Lagrangian density [10]

$$\begin{aligned} \mathcal{L}_{QMC} = & \bar{\psi}(\vec{r}) \left[ i \gamma \cdot \partial - m_N + g_\sigma (\sigma(\vec{r})) \sigma(\vec{r}) \right. \\ & - g_\omega \omega(\vec{r}) \gamma_0 - g_\rho \frac{\tau_3^N}{2} b(\vec{r}) \gamma_0 \\ & \left. - \frac{e}{2} (1 + \tau_3^N) A(\vec{r}) \gamma_0 \right] \psi(\vec{r}) \\ & - \frac{1}{2} [(\nabla \sigma(\vec{r}))^2 + m_\sigma^2 \sigma(\vec{r})^2] \\ & + \frac{1}{2} [(\nabla \omega(\vec{r}))^2 + m_\omega^2 \omega(\vec{r})^2] \\ & + \frac{1}{2} [(\nabla b(\vec{r}))^2 + m_\rho^2 b(\vec{r})^2] + \frac{1}{2} (\nabla A(\vec{r}))^2, \quad (1) \end{aligned}$$

where  $\psi(\vec{r})$ ,  $\sigma(\vec{r})$ ,  $\omega(\vec{r})$ ,  $b(\vec{r})$ , and  $A(\vec{r})$  are the nucleon,  $\sigma$ ,  $\omega$ ,  $\rho$ , and Coulomb fields, respectively. Note that only the time components of the  $\omega$  (a vector-isoscalar meson) and the neutral  $\rho$  (a vector-isovector meson) are kept in the mean-field approximation. These five fields now depend on position  $\vec{r}$ , relative to the center of the nucleus. The spatial distributions are determined by solving the equations of motion self-consistently. The key difference between QMC and quantum hadrodynamics (QHD) [14] lies only in the  $\sigma NN$  coupling constant,  $g_\sigma(\sigma(\vec{r}))$ , which depends on the scalar field in QMC, while it remains constant in QHD. (In practice this is well approximated by  $g_\sigma[1 - (a_N/2)g_\sigma\sigma(r)]$ .) The coupling constants  $g_\sigma$ ,  $g_\omega$ , and  $g_\rho$  are fixed to reproduce the saturation properties and the bulk symmetry energy of nuclear matter. The only free parameter,  $m_\sigma$ , which controls the range of the attractive interaction, and therefore affects the nuclear surface slope and its thickness, is fixed by fitting the experimental rms charge radius of  $^{40}\text{Ca}$ , while keeping the ratio  $g_\sigma/m_\sigma$  fixed, as constrained by the properties of nuclear matter.

The quark wave function, as well as the nucleon wave function (both are Dirac spinors), are determined once a so-

lution to equations of motion are found in a self-consistent way. The electric and magnetic form factors for a bound proton, in the local-density approximation, are simply given by

$$G_{E,M}^\alpha(Q^2) = \int G_{E,M}(Q^2, \rho_B(\vec{r})) \rho_{p\alpha}(\vec{r}) d\vec{r}, \quad (2)$$

where  $\alpha$  denotes a specified orbit with appropriate quantum numbers, and  $G_{E,M}(Q^2, \rho_B(\vec{r}))$  is the density-dependent form factor of a ‘‘proton’’ immersed in nuclear matter with local baryon density,  $\rho_B(\vec{r})$ .<sup>1</sup> One might question the local-density approximation in Eq. (2) and ask whether it would be more appropriate to use the density-dependent form factor for a ‘‘proton’’ immersed in nuclear matter with the corresponding scalar field strength,  $g_\sigma(\sigma(\vec{r}))\sigma(\vec{r})$ . This would correspond to a ‘‘local  $\sigma$  approximation.’’ We have verified that our results are not sensitive to such a change. We calculated the local quantity,  $g_\sigma(\sigma(\vec{r}))\sigma(\vec{r})$ , in the full calculation and compared it to its value calculated within a local-density approximation using  $\rho_B(\vec{r})$ . In <sup>40</sup>Ca the change was less than 5%, while in <sup>208</sup>Pb the change was even less. Thus the two approximations give very similar results and lend support to the present approach.

In terms of the nucleon shell-model wave functions, the local baryon density and the local proton density in the specified orbit  $\alpha$  are easily evaluated as

$$\rho_B(\vec{r}) = \sum_{\alpha}^{\text{occ}} d_{\alpha} \psi_{\alpha}^{\dagger}(\vec{r}) \psi_{\alpha}(\vec{r}),$$

$$\rho_{p\alpha}(\vec{r}) = \left( t_{\alpha} + \frac{1}{2} \right) \psi_{\alpha}^{\dagger}(\vec{r}) \psi_{\alpha}(\vec{r}), \quad (3)$$

where  $d_{\alpha} = (2j_{\alpha} + 1)$  refers to the degeneracy of nucleons occupying the orbit  $\alpha$  and  $t_{\alpha}$  is the eigenvalue of the isospin operator,  $\tau_3^N/2$ . Notice that the quark wave function depends only on the surrounding baryon density. Therefore, this part of the calculation of  $G_{E,M}(Q^2, \rho_B(\vec{r}))$  is the same as in our previous publication for nuclear matter [8].

The notable medium modifications of the quark wave function inside the bound ‘‘nucleon’’ in QMC include a reduction of its eigenfrequency and an enhancement of the lower component of its Dirac spinor. As in earlier work, the corrections arising from recoil and center-of-mass motion for the bag are taken into account using the Peierls–Thouless projection method, combined with Lorentz contraction of the internal quark wave function and with the perturbative pion cloud added afterwards [16]. Note that possible off-shell effects [17] and meson exchange currents [6] are ignored in the present approach. The resulting nucleon electromagnetic form factors agree with experiment quite well in free space

<sup>1</sup>In a more sophisticated treatment, for example, using a full distorted wave calculation, the weighting may emphasize the nuclear surface somewhat more [15].

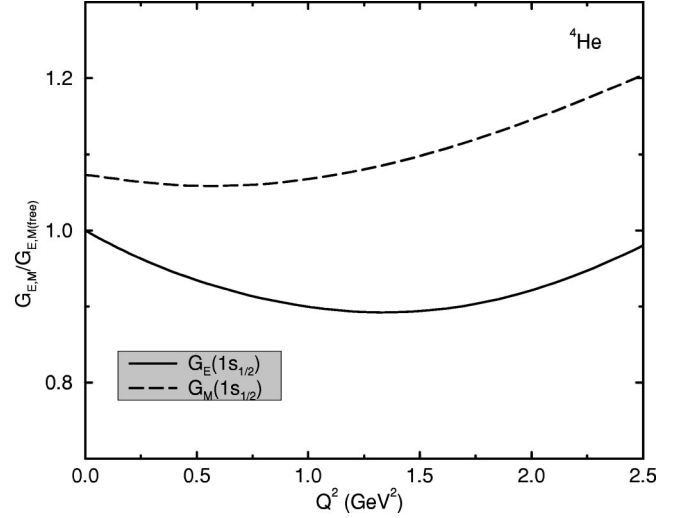


FIG. 1. Ratio of in-medium to free space electric and magnetic form factors for the proton in <sup>4</sup>He. (The free bag radius was taken to be  $R_0 = 0.8$  fm in all figures.)

[16]. Because of the limitations of the bag model the form factors are expected to be most reliable at low momentum transfer (say, less than 1 GeV<sup>2</sup>). To cut down theoretical uncertainties and highlight the deviation from the free nucleon form factors, we prefer to show the ratios of the form factors with respect to corresponding free space values. Throughout this work, we use the renormalized  $\pi NN$  coupling constant,  $f_{\pi NN}^2 \approx 0.0771$  [18]. The bag radius in free space is taken to be 0.8 fm and the current quark mass is 5 MeV in the following figures.

Figure 1 shows the ratio of the proton electric and magnetic form factors for <sup>4</sup>He (which has only one state,  $1s_{1/2}$ ) with respect to the free space values. As expected, both the electric and magnetic rms radii become slightly larger, while the magnetic moment of the proton increases by about 7%. Figure 2 shows the ratio of the proton electric and magnetic form factors for <sup>16</sup>O with respect to the free space values, which has one  $s$  state,  $1s_{1/2}$ , and two  $p$  states,  $1p_{3/2}$  and  $1p_{1/2}$ . The form factors in small  $Q^2$  for the  $s$  orbit nucleon is somewhat more suppressed than those in the  $p$  orbit as the nucleon at the inner orbit experiences a larger average baryon density. The magnetic moment for the  $s$  orbit nucleon is similar to that in <sup>4</sup>He, but it is reduced by 2–3% in the  $p$  orbit. Since the difference between two  $p$  orbits is rather small, we do not plot the results for  $1p_{1/2}$ . For comparison, we also show in Fig. 2 the corresponding ratio of form factors (those curves with triangle symbols) using a variant of QMC where the bag constant  $B$  is allowed to decrease by 10% at the normal nuclear matter density,  $\rho_0$  [19]. It is evident that the effect of a possible reduction in  $B$  is quite large and will severely reduce the electromagnetic form factors for a bound nucleon since the bag radius is quite sensitive to the value of  $B$ .

From the experimental point of view, it is more reliable to show the ratio,  $G_E/G_M$ , since it can be derived directly from the ratio of transverse to longitudinal polarization of the outgoing proton, with minimal systematic errors. We find

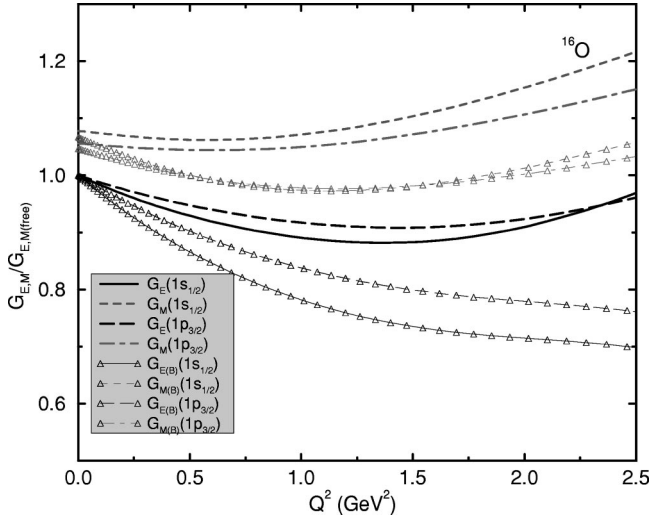


FIG. 2. Ratio of in-medium to free space proton electric and magnetic form factors for the  $s$  and  $p$  shells of  $^{16}\text{O}$ . The curves with triangle symbols represent the corresponding ratio calculated in a variant of QMC with a 10% reduction of the bag constant  $B$  at  $\rho_0$ .

that  $G_E/G_M$  runs roughly from 0.41 at  $Q^2=0$  to 0.28 and 0.20 at  $Q^2=1$  and  $2 \text{ GeV}^2$ , respectively, for a proton in the  $1s_{1/2}$  orbit in  $^4\text{He}$  or  $^{16}\text{O}$ . The ratio of  $G_E/G_M$  with respect to the corresponding free space ratio is presented in Fig. 3. The results for the  $1s_{1/2}$  orbit in  $^{16}\text{O}$  and  $^4\text{He}$  are similar and are roughly 2% lower than that for the  $p$  orbits in  $^{16}\text{O}$ . With a smaller  $B$ , this ratio of ratios drops quickly as  $Q^2$  increases.

For completeness, we have also calculated the electromagnetic form factors for the bound nucleon in heavy nuclei such as  $^{40}\text{Ca}$  and  $^{208}\text{Pb}$ . The form factors for the proton in selected shell orbits are shown in Fig. 4. Because of the larger central baryon density of heavy nuclei, the proton electric and magnetic form factors in the inner orbits ( $1s_{1/2}$ ,  $1p_{3/2}$ , and  $1p_{1/2}$  orbits) suffer much stronger medium modi-

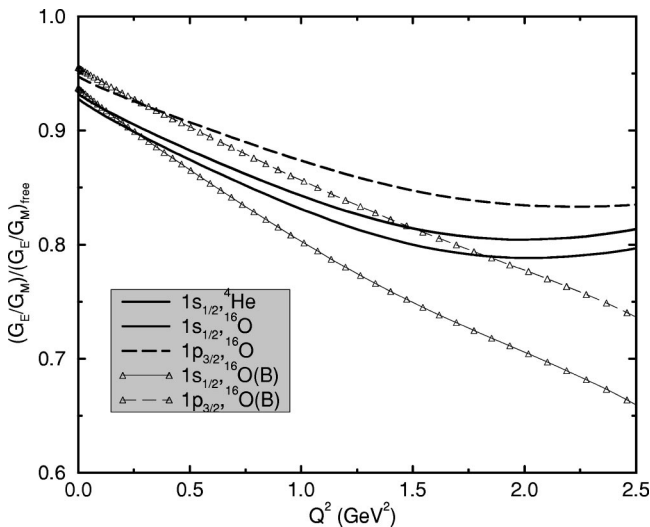


FIG. 3. Ratio of in-medium proton electric to magnetic form factors with respect to the free space ratio. As in the previous figure, curves with triangle symbols represent the corresponding results calculated in a variant of QMC with a 10% reduction of  $B$  at  $\rho_0$ .

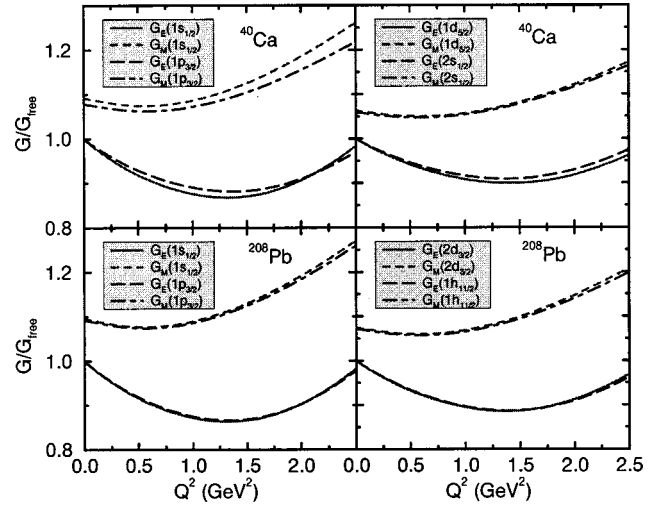


FIG. 4. Ratio of in-medium to free space electric and magnetic form factors in specific orbits, for  $^{40}\text{Ca}$  and  $^{208}\text{Pb}$ .

fications than those in light nuclei. That is to say, the  $Q^2$  dependence is further suppressed, while the magnetic moments appear to be larger. Surprisingly, the nucleons in peripheral orbits ( $1d_{5/2}$ ,  $2s_{1/2}$ , and  $1d_{3/2}$  for  $^{40}\text{Ca}$  and  $2d_{3/2}$ ,  $1h_{11/2}$ , and  $3s_{1/2}$  for  $^{208}\text{Pb}$ ) still show significant medium effects, comparable to those in  $^4\text{He}$ .

Finally, we would like to add some comments on the magnetic moment in a nucleus. In the present calculation, we have only calculated the contribution from the intrinsic magnetization (or spin) of the nucleon, which is modified by the scalar field in a nuclear medium [20]. As shown in the figures we have found that the intrinsic magnetic moment is enhanced in matter because of the change in the quark structure of the nucleon. We know, however, that there are several, additional contributions to the nuclear magnetic moment, such as meson exchange currents, higher-order correlations, etc. As is well known in relativistic nuclear models like QHD, there is a so-called magnetic moment problem in the mean-field approximation [21]. To cure this problem, one must calculate the convection current matrix element within the relativistic random-phase approximation (RRPA) [22]. However, at high momentum transfer we expect that it should be feasible to detect the enhancement of the intrinsic spin contribution which we have predicted because the long-range correlations, like RRPA, should decrease much faster in that region.

In summary, we have calculated the electric and magnetic form factors for the proton, bound in specific shell-model orbits, for several closed-shell, finite nuclei. Generally the electromagnetic rms radii and the magnetic moments of the bound proton are increased by the medium modifications. Though the difference between the proton form factors for shell orbits split by the spin-orbit force is very small, the difference between inner and peripheral orbits is considerable. It is worthwhile to point out that this medium correction is solely due to the change of the internal quark structure, while a complete description of the experiment (in terms of response functions or nuclear form factors) may still require further many-body effects. In view of current experi-

mental developments, particularly the ability to precisely measure electron-nucleus quasielastic scattering polarization observables, it should be possible to detect differences between the form factors in different shell-model orbits. The current and future experiments at TJNAF and Mainz, therefore, promise to provide vital information with which to

guide and constrain dynamic microscopic models for finite nuclei, and perhaps unambiguously isolate a signature for the role of quarks.

We would like to acknowledge useful discussions with C. Glashauser and J. J. Kelly. This work was supported by the Australian Research Council.

- 
- [1] For an overview, see e.g., *Quark Matter '95*, Nucl. Phys. **A590**, (1995).
- [2] J. J. Aubert *et al.*, Phys. Lett. **123B**, 275 (1983); R. G. Arnold *et al.*, Phys. Rev. Lett. **52**, 727 (1984); D. F. Geesaman, K. Saito, and A. W. Thomas, Annu. Rev. Nucl. Part. Sci. **45**, 337 (1995).
- [3] B. Buck and S. M. Perez, Phys. Rev. Lett. **50**, 1975 (1983).
- [4] R. Artemus *et al.*, Phys. Rev. Lett. **44**, 965 (1980); R. Barreau *et al.*, Nucl. Phys. **A402**, 515 (1983).
- [5] P. J. Mulders, Phys. Rep. **185**, 83 (1990); H. Kurasawa and T. Suzuki, Phys. Lett. B **208**, 160 (1988).
- [6] W. M. Alberico, T. W. Donnelly, and A. Molinari, Nucl. Phys. **A512**, 541 (1990); J. W. Van Orden and T. W. Donnelly, Ann. Phys. (N.Y.) **131**, 451 (1981); W. M. Alberico, M. Ericson, and A. Molinari, *ibid.* **154**, 356 (1984).
- [7] Ulf-G. Meissner, Phys. Lett. B **220**, 1 (1989); Ulf-G. Meissner, Phys. Rev. Lett. **27**, 1013 (1989); E. Ruiz Arriola, Chr. V. Christov, and K. Goeke, Phys. Lett. B **225**, 22 (1989); Chr. V. Christov, E. Ruiz Arriola, and K. Goeke, Nucl. Phys. **A510**, 689 (1990); Il-T. Cheon and M. T. Jeong, J. Phys. Soc. Jpn. **61**, 2726 (1992).
- [8] D. H. Lu, A. W. Thomas, K. Tsushima, A. G. Williams, and K. Saito, Phys. Lett. B **417**, 217 (1998); D. H. Lu, A. W. Thomas, K. Tsushima, A. G. Williams, and K. Saito, *ibid.* **441**, 27 (1998).
- [9] P. A. M. Guichon, Phys. Lett. B **200**, 235 (1988); S. Fleck, W. Bentz, K. Shimizu, and K. Yazaki, Nucl. Phys. **A510**, 731 (1990).
- [10] K. Saito, K. Tsushima, and A. W. Thomas, Phys. Rev. C **55**, 2637 (1997); P. A. M. Guichon, K. Saito, E. Rodionov, and A. W. Thomas, Nucl. Phys. **A601**, 349 (1996); K. Saito, K. Tsushima, and A. W. Thomas, *ibid.* **A609**, 339 (1996).
- [11] I. Sick, in *Proceedings of the International Conference on Weak and Electromagnetic Interactions in Nuclei*, edited by H. Klapdor (Springer-Verlag, Berlin, 1986), p. 415; I. Sick, Comments Nucl. Part. Phys. **18**, 109 (1988); D. B. Day, J. S. McCarthy, T. W. Donnelly, and I. Sick, Annu. Rev. Nucl. Part. Sci. **40**, 357 (1990).
- [12] J. Jourdan, Phys. Lett. B **353**, 189 (1995); Nucl. Phys. **A603**, 117 (1996).
- [13] G. Glashauser, CEBAF/89-033; (private communication); D. Abbott *et al.*, Phys. Rev. Lett. **80**, 5072 (1998).
- [14] J. D. Walecka, Ann. Phys. (N.Y.) **83**, 497 (1974); B. D. Serot and J. D. Walecka, Adv. Nucl. Phys. **16**, 1 (1986).
- [15] J. J. Kelly (private communication).
- [16] D. H. Lu, A. W. Thomas, and A. G. Williams, Phys. Rev. C **55**, 3108 (1997); **57**, 2628 (1998).
- [17] T. De Forest, Jr., Nucl. Phys. **A392**, 232 (1983); H. W. L. Naus and J. H. Koch, Phys. Rev. C **36**, 2459 (1987); H. W. L. Naus, S. J. Pollock, J. H. Koch, and U. Oelfke, Nucl. Phys. **A509**, 717 (1990).
- [18] D. V. Bugg and R. Machleidt, Phys. Rev. C **52**, 1203 (1995).
- [19] D. H. Lu, K. Tsushima, A. W. Thomas, A. G. Williams, and K. Saito, Nucl. Phys. **A634**, 443 (1998).
- [20] K. Saito and A. W. Thomas, Phys. Rev. C **51**, 2757 (1995).
- [21] J. D. Walecka, *Theoretical Nuclear and Subnuclear Physics* (Oxford University Press, Oxford, 1995).
- [22] H. Kurasawa and T. Suzuki, Phys. Lett. **165B**, 234 (1985).